NEOPLASIA
www.neoplasia.com

Volume 17 Number 11 November 2015 pp. 826–838 826

Epigenetic Regulation of GDF2 Suppresses Anoikis in Ovarian and Breast Epithelia[1]

Archana Varadaraj*, Pratik Patel*,[2], Anne Serrao*,[2], Tirthankar Bandyopadhay*, Nam Y. Lee[‡,§], Amir A. Jazaeri[¶], Zhiqing Huang[#], Susan K. Murphy[#] and Karthikeyan Mythreye*,[†]

*Department of Chemistry and Biochemistry, University of South Carolina, Columbia SC 29208; [†]Department of Drug Discovery and Biomedical Sciences, South Carolina College of Pharmacy, SC; [‡]Division of Pharmacology, College of Pharmacy, Columbus, OH 43210; [§]Davis Heart and Lung Research Institute, Columbus, OH 43210; [¶]Department of Gynecologic Oncology and Reproductive Medicine, University of Texas MD Anderson Cancer Center; [#]Department of Gynecology and Oncology, Duke University, Durham NC 29210

Abstract

Anoikis, a cell death mechanism triggered upon cell-matrix detachment, is regarded as a physiological suppressor of metastasis that can be regulated by a diverse array of signals. The protein encoded by *GDF2* is BMP9 and is a member of the bone morphogenetic protein family and the transforming growth factor (TGF) β superfamily with emerging yet controversial roles in carcinogenesis. In an attempt to identify the function of growth and differentiation factor 2 (GDF2) in epithelial systems, we examined the signaling machinery that is involved and cell fate decisions in response to GDF2 in ovarian and breast epithelia. We find that GDF2 can robustly activate the SMAD1/5 signaling axis by increasing complex formation between the type I receptor serine threonine kinases activin receptor-like kinase (ALK) 3 and ALK6 and the type II receptor serine threonine kinase BMPRII. This activation is independent of cross talk with the SMAD2-transforming growth factor β pathway. By activating SMAD1/5, epithelial cells regulate anchorage-independent growth by increasing anoikis sensitivity that is dependent on GDF2's ability to sustain the activation of SMAD1/5 via ALK3 and ALK6. Consistent with a role for GDF2 in promoting anoikis susceptibility, the analysis of cell lines and patient data suggests epigenetic silencing of *GDF2* in cancer cell lines and increased promoter methylation in patients. These findings collectively indicate an antimetastatic role for GDF2 in ovarian and breast cancer. The work also implicates loss of GDF2 via promoter methylation-mediated downregulation in promotion of carcinogenesis with significant relevance for the use of epigenetic drugs currently in clinical trials.

Neoplasia (2015) 17, 826–838

Introduction

Transforming growth factor (TGF)-β superfamily members play distinct roles in tumorigenesis, acting to promote advanced-stage cancers whilst inhibiting the early events in the processes that lead up to it [1]. BMP9, also known as growth and differentiation factor 2 (GDF2), and BMP10 form a subgroup within the TGF-β superfamily based on similarities in their primary amino acid sequences and overlapping functions in the context of angiogenesis [2–4]. Although the roles of GDF2 as an inducer and inhibitor of

Address all correspondence to: K. Mythreye, Department of Chemistry and Biochemistry, 631 Sumter St, University of South Carolina, Columbia SC 29208.
E-mail: Mythreye@sc.edu

[1]This work was funded in part by the Ovarian Cancer Research Fund grant # 258785, NIGMS/COBRE grant 5P20GM109091-02 to K. M., and the Gail Parkins Ovarian Cancer Awareness fund for S. K. M.
[2]Equal contribution.
Received 4 August 2015; Revised 2 November 2015; Accepted 8 November 2015

1476-5586
http://dx.doi.org/10.1016/j.neo.2015.11.003

neovascularization and angiogenesis have been well studied [5–8] there is little insight into the functions of GDF2 in cancers of epithelial origin. The relevance of GDF2 signaling in nonendothelial cells stems from the finding that GDF2 is expressed in the liver, mediates ectopic bone growth [9], is a differentiation factor for cholinergic neurons of the central nervous system [10], and induces proliferation of cultured cells [11–13]. Studies in hepatocytes have shown that GDF2 is proliferative in transformed cells with no changes in proliferative capacity of immortalized hepatocytes [13]. Additionally, GDF2 has also been shown to suppress breast cancer *in vivo* [14].

GDF2 signaling in endothelial cells is initiated upon its binding to the heteromeric type I/type II receptor. Two different type I receptor serine threonine kinases have been implicated in GDF2 signaling: activin receptor-like kinase (ALK) 1 in endothelial cells [5,15] and ALK2 in other cell types [5,13,16]. Three type II receptors are part of the GDF2 signaling complex: BMP type II receptor (BMPRII) and activin type II receptors A and B (ActRIIA and ActRIIB) [5,16]. However, type I and type II receptor specificity maybe cell type dependent, involving more than one type I [5] or type II receptors [16]. Receptor activation upon ligand binding then activates the receptor regulated SMADs (R-SMAD) SMAD1, SMAD5, and SMAD8, allowing complex formation with the co-SMAD SMAD4, nuclear translocation of the complex, and target gene regulation [17].

Ovarian and breast cancers are the two most lethal of women's cancers. In HER2-positive breast cancer cells, GDF2 treatment has been shown to decrease HER2 protein and transcript levels and reduce tumor volume in nude mice [18]. In contrast, GDF2 has been shown to mediate pro-proliferative effects through the ALK2/SMAD1/SMAD4 pathway in epithelial ovarian cancer cells [16]. Although there is very little known about the specific mechanisms of GDF2 signaling in breast cancer, there is also a gap in the understanding of GDF2 function in ovarian cancers. Contrary to our notion of the origin of ovarian cancer, a systematic study of the pathology of non-neoplastic tubular cells of the fimbriae in women with familial BRCA1/2 mutations revealed the significance of the tubular cells as the site of onset for serous ovarian carcinoma [19]. The transformation of primary human fallopian tube epithelial cells (FTECs) and its subsequent injection in SCID mice have also demonstrated the indistinguishable histology and transcriptional profile between the xenograft and cells from patient-derived serous ovarian cancer [20]. Thus, the protumorigenic or antitumorigenic potential of GDF2 in experimental conditions of breast and ovarian cancer that closely mimics physiological states of disease is still a subject of critical relevance. In addition, the contribution of the transformation status to GDF2-mediated mechanisms of cancer evasion also remains unexplored.

In this study, we investigate the biological outcome of GDF2 signaling in normal and transformed breast and FTECs. We show that functional GDF2 signaling as seen from SMAD1/5 phosphorylation, nuclear translocation, and ID1 target gene expression occurs via ALK3 and ALK6 type I receptors in cell lines with relatively high ALK3 and ALK6 levels. We also show that in the presence of equal amounts of ALK2, ALK3, and ALK6, GDF2 specifically potentiates binding between ALK3 and ALK6 with the type II receptor BMPRII. Interestingly, although we do not find a significant change in cell proliferation upon GDF2 treatment, GDF2 significantly enhances anoikis/anchorage independent growth via the ALK3/ALK6/SMAD1 axis. Reducing the activity of ALK3, ALK6, or SMAD1 abrogates GDF2-dependent anoikis sensitivity, thereby demonstrating the requirement of intact ALK3 and ALK6 signaling to SMAD1/5 to confer anoikis sensitivity in ovarian and breast epithelial cells. We find that reduced GDF2 protein levels in several cancer lines are consistent with *GDF2* promoter methylation observed in ovarian cancer patients compared with normal counterparts. Bisulfite sequencing confirmed that GDF2 promoter methylation and demethylation correlated with reexpression of GDF2 in transformed cells, implicating epigenetic silencing of the GDF2 pathway in cancer.

Materials and Methods

Cell Lines and Culture Conditions

Normal FTECs P210 and P211 and the transformed FTEC P76 were generated as described [20]. Ovarian teratoma and epithelial carcinoma cell lines PA1, SKOV3, and OVCA429 were obtained from Duke Gynecology/Oncology Bank, and the immortalized ovarian surface epithelial cells IOSE80 and IOSE144 were obtained from Canadian Ovarian Tissue Bank. Authentication of the cell lines from the Duke Gynecology/Oncology Bank was carried out at the UC Denver sequencing facility. All other cell lines used in this study were obtained from ATCC.

FTECs: P210, P211, P76, murine mammary carcinoma cell line: 67NR, 4T1, and HEK293 cells were grown in complete DMEM supplemented with L-glutamine, 10% fetal bovine serum (FBS) and 100 U of penicillin-streptomycin. Epithelial carcinoma cell lines: PA1, SKOV3, and OVCA429 were cultured in RPMI containing L-glutamine, 10% FBS, and 100 U of penicillin-streptomycin. The normal human mammary epithelial cell line MCF10A was cultured in F12/DMEM (1:1) supplemented with 5% horse serum, 10 μg/ml of insulin, 0.5 μg/ml of hydrocortisone, 20 ng/ml of EGF, and 100 ng/ml of cholera toxin. Human mammary epithelial cell (HMEC) lines were grown in complete HMEC media containing bovine pituitary extract (Clonetech#CC-2551). Immortalized ovarian surface epithelial cells IOSE80 and IOSE144 were maintained in M199:MCDB105 medium (Invitrogen #11150, Sigma #M6395) with 5% FBS. All cells lines were maintained at 37°C in a humidified incubator at 5% CO_2.

Antibodies, Reagents, and Plasmids

Antibodies phosphoSMAD1/5 (#9516S), BMPRII (#6979), cleaved caspase 3 (#9661), caspase 3 (#9662), BIM (#2819), HA-Tag rabbit (#C29F4), and SMAD1 (#6944S) were from Cell Signaling Technology. Total SMAD1/5 (#sc-6201), ID1 (#365654), and GDF2 (#130703) were from Santa Cruz Biotech. Actin (#A2228) was from Sigma, and anti-HA antibody (#32-6700) was from Invitrogen. Inhibitors SB431542 hydrate (#S4317), dorsomorphin (#p5499), 5-azacytidine (#A2385), TAK inhibitor 5 Z-7-oxozeaenol (#O9890), and trichostatin A (#T8552) were from Sigma. ALK1/2 inhibitor ML347 (#4945) was from Tocris Bioscience. Pan-caspase inhibitor z-vad-fmk (#fmk001), Alk1-ECD (#370-AL-100), TGFβ, BMP2, GDF2, and BMP10 were from R&D Systems. Constructs expressing ALK2-Flag, ALK3-HA, ALK6-HA, ALK3 (KR)-HA and ALK6 (KR)-HA, BRE-Luc, PE2.1, and P3TP were a kind gift from Miyazono K. [21]. shRNA constructs to ALK2, ALK3, ALK6, and BMPRII were obtained from Sigma (Supplementary Table 1*A*). For SMAD1 knockdown, PA1 cells were infected with 100 MOI of SMAD1 shRNA adenovirus construct, generously provided by Maria Trojanowska. Q-PCR primer sequences and primers designed to the CpG1 site of the

GDF2 promoter are listed in Supplementary Table 1, *B* and *C*. Lipofectamine 2000 (#11668019) was from Life Technologies, and Duolink to measure proximity ligation was from OLink Bioscience. Caspase-Glo 3/7 Assay System (Promega #G8090) and MTT reagent were obtained from Amresco.

Luciferase Assay

Cells were transfected with the BRE-Luc reporter plasmid. Treatment with BMP4 (10 nM) or GDF2 (10 ng/ml) was carried out for 24 hours after 6 hours of serum starvation. Cells were collected and lysed in 1× passive lysis buffer (Promega) according to manufacturer's instructions. To measure luciferase activity, 20 µl of lysate was added to 25 µl of Luciferase Assay Reagent (Promega), and luminescence was quantitated using a luminometer (Biotek). Where indicated, dorsomorphin treatment concentrations were at 3 µM.

Cell Lysis and Immunoprecipitation

Cells were lysed in SDS lysis buffer for immunoblot analysis. For co-immunoprecipitation, HEK293 cells were lysed in nondenaturing E1A lysis buffer (50 mM HEPES pH 7.5, 150 mM of NaCl, 0.1% Nonidet P-40, 0.2 mM PMSF, 1 mg/ml of aprotin, and 1 mg/ml of leupeptin).

Anoikis Assay

For anoikis assay, 400,000 cells were plated on poly-HEMA–coated 12-well plates. Cells were harvested at specified times following treatment with GDF2, washed with 1× PBS, and lysed for immunoblot analysis. For the MTT assay, cells grown on poly-HEMA–coated plates for the indicated times were collected and reseeded on tissue culture plates and allowed to reattach overnight, and MTT solution at a final concentration of 1 mM was added. The plates were incubated in a 37°C incubator for 2 to 3 hours, DMSO was added to dissolve the formazan crystals, the supernatant was pipetted in triplicates in a 96-well plate, and absorbance measured using a Synergy HT plate reader at 570 nm. Caspase-Glo Assay to quantify active caspase 3/7 was carried out according to manufacturer's instructions (Promega #G8090).

GDF2 ELISA

The GDF2 ELISA was performed according to manufacturer's instructions (R&D Systems, #Dy3209). Briefly, 90,000 cells were plated in triplicate in a 96-well plate. After the cells adhered to the plate, medium was replaced to serum-free medium, and the assay procedure was initiated after overnight incubation in serum-free medium. GDF2 standards ranged from 15 to 1000 pg/ml, and absorbance values were calculated from the difference between OD 450 nm and OD 570 nm to account for plate correction.

Growth of MCF10A Acini in Matrigel

The protocol for the growth of MCF10A acini was as previously described [22]. Briefly, cells were seeded on Matrigel-coated chamber slides in media containing 2% Matrigel in the presence or absence of 20 ng/ml of GDF2 treatment or in the presence or absence of 20 µM z-vad-fmk. Acini growth was monitored and documented at day 10.

Immunofluorescence and Microscopy

Cells were fixed in 4% paraformaldehyde, permeabilized in 0.3% TX-100, and blocked with 1% BSA PBS. Primary antibody (1:200) incubation for an hour was followed by 30-minute incubation with Alexa Fluor 488 (H+L) (#A11008 Life Technologies). After washing, cells were stained with 4′6-diamidino-2-phenylindole (Roche). *In situ* proximity ligation assay was carried out according to manufacturer's instructions. Imaging and *z*-stacking were performed using a Zeiss LSM700 confocal microscope.

Quantitative Polymerase Chain Reaction (qRT-PCR)

For qRT-PCR, total RNA was isolated from approximately 200,000 cells using Trizol reagent (Invitrogen, Carlsbad, CA). RNA was retrotranscribed using the 5× reaction mix (#R1362, Thermo Scientific) and the Maxima Enzyme Mix (#K1642, Thermo Scientific). qRT-PCR primer sequences are listed in Supplementary Table 1B.

GDF2 Promoter Methylation Analysis

GDF2 promoter methylation from genomic DNA obtained from patient samples was validated as described [23]. Bisulfite sequencing to quantify methylation at the CpG site within the GDF2 promoter was carried out as previously described [24]. Briefly, bisulfite conversion was performed with 800 ng of DNA. PCR and pyrosequencing assay were designed and performed using Qiagen PyroMark assay design software and kit (Supplementary Table 1*C*). The assay was validated with different proportions of methylated and unmethylated DNA, and the correlation curve (R^2 = 0.98) was generated and compared with the input (data not shown).

Results

BMP9/GDF2 and not BMP10 activates SMAD1/5 in both normal and oncogenic Ovarian and Breast epithelial Cells

Given that GDF2 and BMP10 have been identified as ALK1 ligands in endothelial cells [6], their role in normal and oncogenic epithelial cells that express low levels of the endothelial specific ALK1 receptor remains unclear [25] (Supplementary Figure S1*A*). To ask whether GDF2 treatment would engage downstream signaling events in nontumorigenic and transformed ovarian and breast epithelial cancer cell lines, a time-course analysis of SMAD1/5 phosphorylation was carried out in a panel of breast and ovarian cell lines. Ovarian surface epithelial cells were previously considered as suitable *in vitro* models of serous ovarian carcinoma, whereas recent work has shown that the molecular determinants that recapitulate the disease arise from tubular cells of the fimbriae [20]. To investigate the response of an experimental model that closely mimics the site of origin of serous carcinoma, we treated immortalized FTEC P211 [20] and the normal breast epithelial cell line MCF10A with GDF2 for the indicated times (Figure 1*A*). An identical pulse of GDF2 was also carried out in the oncogenic P76, an FTEC line transformed with an oncogenic cocktail [20], in the ovarian teratoma cancer cell line PA1 isolated from ascites [26] and in the breast cancer lines 4T1 and 67NR. Robust SMAD1/5 phosphorylation was seen as early as 15 minutes after GDF2 treatment (Figure 1, *A* and *B*). A dose course with GDF2 also confirmed the sensitivity of the epithelial cell lines to GDF2 signaling (Supplementary Figure S1, *B* and *C*). Because prior studies have indicated that BMP superfamily members (BMP2/4) can activate the SMAD2/3 pathways as well [27], we examined SMAD2/3 signaling in these cell lines. Whereas TGF-β activated SMAD2/3 in 30 minutes, GDF2 did not phosphorylate SMAD2/3 and did not activate the CAGA promoter specific for TGFβ-induced SMAD2/3 activation (Supplementary Figure S1, *D* and *E*). Thus, GDF2 led exclusively to SMAD1/5 phosphorylation.

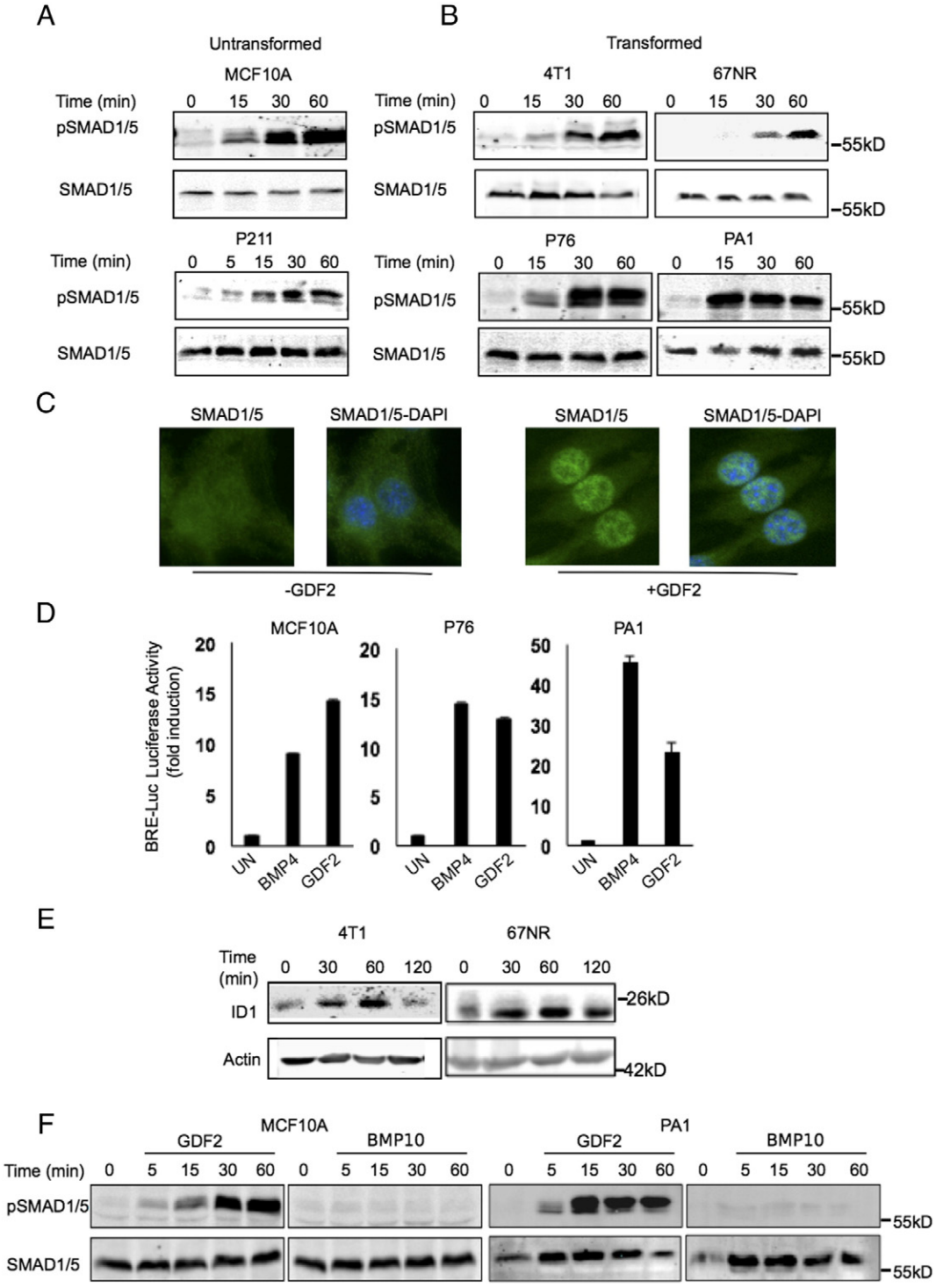

Figure 1. GDF2 activates SMAD1/5 in breast and ovarian epithelial cells. (A) Western blotting of lysates from untransformed breast (MCF10A) and FTEC line FTEC 211 treated with GDF2 (10 ng/ml) for the indicated times and immunoblotted for pSMAD1/5 and SMAD1/5. (B) Western blotting of lysates from transformed breast cancer lines 4T1 and 67NR including the transformed oncogenic FTEC P76 and ovarian cancer line PA1 treated as in (A) and immunoblotted for pSMAD1/5 and total SMAD1/5. (C) SMAD1/5 translocates to the nucleus. Immunofluorescence images of 4T1 cells treated with GDF2 for 30 minutes followed by immunostaining for SMAD1/5. Overlay images are shown with the nuclear stain 4′6-diamidino-2-phenylindole. (D) GDF2 specifically induces BRE-luciferase promoter activity. Luciferase activity (Methods) of either BMP4 (10 nM)– or GDF2 (10 ng/ml)–treated MCF10A, p76, and PA1 cells as indicated normalized to untreated cells is presented. (E) ID1 target protein expression. Western blotting for ID1 in 4T1 and 67NR cells treated with GDF2 at indicated time points. Loading control was actin. (F) pSMAD1/5 phosphorylation in response to BMP10 is less robust compared with GDF2. Western blotting of MCF10A and PA1 lysates treated with 10 ng/ml of GDF2 or BMP10 for the indicated times.

Consistent with SMAD1/5 activation in response to GDF2, we observed distinct nuclear translocation of SMAD1/5 (Figure 1*C*) and the activation of the BMP response element (BRE-Luc) [28] in response to GDF2 treatment (Figure 1*D*). In accordance with promoter activity, protein levels of ID1, a direct target of BMPs [29], also increased upon GDF2 treatment (Figure 1*E*).

Because BMP10 is most closely related to GDF2 among the GDF/BMP family, we also investigated the activation of SMAD1/5 phosphorylation in response to BMP10. Little to no activation of SMAD1/5 phosphorylation was seen upon BMP10 treatment in two independent cell lines (Figure 1*F*). These data suggest that GDF2 is a robust activator of SMAD1/5 in epithelial cells, causes nuclear translocation of SMAD1/5, and induces SMAD1 target gene and protein expression in both breast and ovarian epithelial cells.

GDF2-induced SMAD1 signaling is mediated via BMPRII-ALK3 and BMPRII-ALK6

TGF-β superfamily members activate signaling by binding and activating specific type I (ALK2, 3,4,5,6,7) and type II serine threonine kinase receptors with the BMP superfamily member initiating signaling through interactions with the type I receptor [30]. Prior studies have indicated cross talk between BMP and the TGF-β receptor serine threonine kinases as well [27]. Thus, to investigate which type I receptor was required for GDF2-induced SMAD1 phosphorylation, we first examined basal expression of type I and type II receptors in the cell lines used. Interestingly, MCF10A cells expressed relatively higher levels of ALK2, whereas all other cell lines examined expressed relatively higher levels of ALK3 (Supplementary Figure S2*A*), a trend that is in accordance with the NCI60 panel of breast and ovarian cancer lines [31,32]. We tested GDF2-induced SMAD1/5 phosphorylation in the presence of dorsomorphin, an inhibitor of ALK2, ALK3, and ALK6 [33], or SB431542, an inhibitor of ALK4, ALK5, and ALK7 [34]. Although treatment with SB431542 clearly inhibited TGFβ-induced SMAD2/3 phosphorylation (Supplementary Figure S2*B*), SMAD1/5 phosphorylation in response to GDF2 was abrogated specifically in the presence of dorsomorphin (Figure 2*A*). Because dorsomorphin blocks ALK2, 3, and 6, we sought to examine the involvement of ALK2 in mediating the SMAD1/5 phosphorylation in response to GDF2. We used ML347, an ALK2 inhibitor with a >300-fold selectivity for ALK2 compared with ALK3 [35]. GDF2-induced SMAD1/5 phosphorylation was dampened by ML347 to a greater extent in MCF10A cells that express high levels of ALK2 (Figure 2*B*, Supplementary Figure S2*C*) compared with SMAD1/5 activation in PA1 cells that express high levels of ALK3 (Figure 2*B*, Supplementary Figure S2*A*). These data confirm prior studies on the roles of ALK2 in mediating GDF2 signaling [16] but, importantly, point to ALK3/ALK6 as being used with equal efficiency to ALK2 by GDF2 to activate SMAD1/5. To confirm the effects of the inhibitors to the type I receptors and to investigate the type II receptor that cooperates with the type I receptor in activating the SMAD1/5 pathway, we independently knocked down ALK2, ALK3, ALK6, and BMPRII using shRNA (Figure 2, *C* and *D*). GDF2-activated SMAD1/5 phosphorylation was abrogated upon reducing expression of ALK3, ALK6, or BMPRII (Figure 2*C*), with a much more modest effect upon loss of ALK2, consistent with our inhibitor experiments (Figure 2, *A* and *B*). As a third approach, to strengthen our findings on the involvement of ALK3 and ALK6 in mediating SMAD1/5 phosphorylation, we carried out a time-course analysis on SMAD1/5 phosphorylation in the presence of ALK3 K-R and ALK6 K-R, the respective kinase-inactive and dominant negative forms of ALK3 and ALK6, [21] in PA1 and MCF10A cells (Figure 2*E*). Both ALK3 K-R and ALK6 K-R were able to effectively reduce SMAD1 phosphorylation following GDF2 treatment in both cell lines (Figure 2*E*).

Consistently, luciferase activity upon GDF2 treatment also showed reduced transcriptional SMAD1/5 response in cells treated with dorsomorphin, confirming the involvement of ALK3 and ALK6 in GDF2-induced SMAD1/5 activation (Figure 2*F*). The inhibitor treatments, shRNA, and mutant approach together indicate a dominant role for ALK3/ALK6 in GDF2-induced SMAD1/5 activation.

GDF2 enhances complex formation between BMPRII-ALK3 and BMPRII-ALK6

Given the role of ALK3, ALK6, and BMPRII in GDF2-induced SMAD activation, we asked whether GDF2 stimulated specific BMPRII interactions with ALK3 and ALK6. Although ALK3 and ALK6 co-immunoprecipitated with endogenous BMPRII at steady state consistent with prior studies demonstrating complex formation between the two receptors at the basal level [36], GDF2 treatment enhanced the interaction between each of the type I receptors (ALK3 and ALK6) and BMPRII (Figure 3, *A* and *B*). To complement the co-immunoprecipitation studies and visualize this interaction, we used a proximity dependent ligation assay [37] to examine and quantify proximity of the two type I receptors and BMPRII in unstimulated and GDF2 stimulated cells. Consistent with the co-immunoprecipitation, ALK3 and ALK6 interaction with endogenous BMPRII was increased in response to GDF2 (Figure 3, *C* and *D*, two-fold $^{**}P < .01$). However, BMPRII and ALK2 interactions were unaffected (Figure 3, *C* and *D*). Thus, GDF2 specifically increased the respective interactions between ALK3 and ALK6 with BMPRII.

GDF2 increases anoikis sensitivity of epithelial cells via ALK3/ALK6/SMAD1

One common cellular event in the initiation and metastasis of breast and ovarian cancer, respectively, is the ability of epithelial cells to become anoikis resistant and overcome anchorage-dependent growth [38,39]. Therefore, we sought to examine if GDF2 provided any survival advantage under anoikis conditions. Using the GDF2 dose that ubiquitously induced SMAD1/5 signaling (10 ng/ml for PA1 and 10-20 ng/ml for 4T1 (Supplementary Figure S1), we find that, in ovarian, breast, and FTECs (PA1 and 4T1 and P76), GDF2 increased anoikis sensitivity (2- to 10-fold) as measured by an increase in cleaved caspase 3 (CC3) levels as early as 6 hours after anchorage-independent growth (Figure 4*A*). In addition, the proapoptotic protein Bim also increased in the presence of GDF2 under anoikis conditions (Supplementary Figure S3*A*). A secondary quantitative approach examining caspase 3/7 activity also indicated a significant increase [40] following GDF2 treatment (Supplementary Figure S3*B*) consistent with the increased CC3 (Figure 4*A*). In addition, cell viability after anoikis in the presence and absence of GDF2 as measured by an MTT assay in two different cell lines (transformed FTEC P76 cells and transformed breast cell line 4T1) also revealed significant decreases in cell viability in response to GDF2 (Figure 4*B*). Because our data collectively point to an increase in anoikis sensitivity following GDF2 treatment, we wanted to investigate the effects on long-term survival and proliferation. Mammary epithelial cells MCF10A form spheroids upon growth in Matrigel [22], and normal morphogenesis triggers anoikis between day 8 and day 10 [22]. To study long-term anchorage-independent

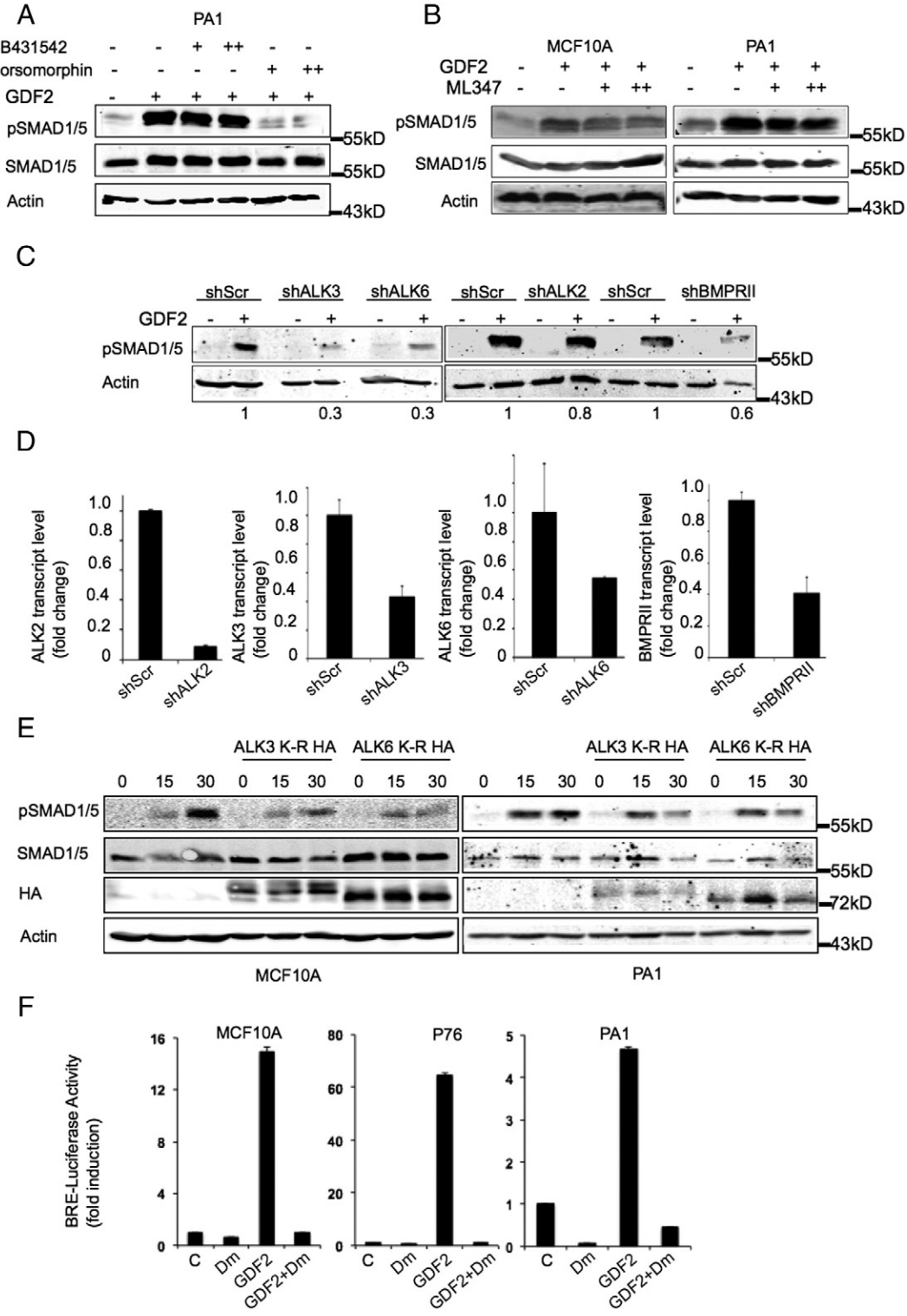

Figure 2. ALK3 and ALK6 are required for GDF2-induced SMAD1/5 phosphorylation. (A-B) Western blotting for pSMAD1/5 activation in PA1 and MCF10A cells in the presence and absence of dorsomorphin 1 μM (+) or 3 μM (++), SB431542 3 μM (+) or 5 μM (++), or ML347 500 nM (+) or 1 mM (++) as indicated with and without GDF2 (10 ng/ml) as indicated (quantification of pSMAD1/5 levels presented in Supplementary Figure S2*C*). (C) Immunoblotting of pSMAD1/5 in PA1 cells in the presence of shRNAs to ALK2, ALK3, ALK6, and BMPRII without and with GDF2 treatment (10 ng/ml) for 30 minutes. (D) QRT-PCR analyses of (C) to confirm reduced expression of ALK2, ALK3, ALK6, and BMPRII expression as indicated. (E) Kinase inactive ALK3 and ALK6 inhibit SMAD1/5 phosphorylation. Western blotting as indicated in MCF10A and PA1 cells in the presence of either mock transfected or HA-tagged kinase inactive ALK3 (ALK3 K-R) or ALK6 (ALK6 K-R) and treated with GDF2 for the time points indicated. Actin was the loading control. (F) Dorsomorphin inhibits SMAD1/5 transcriptional activation. BRE-luciferase reporter activity in indicated cells in the absence (GDF2 alone) or presence of 1 μM dorsomorphin (GDF2+DM). Fold induction of luciferase activity compared with DMSO-treated control cells is presented.

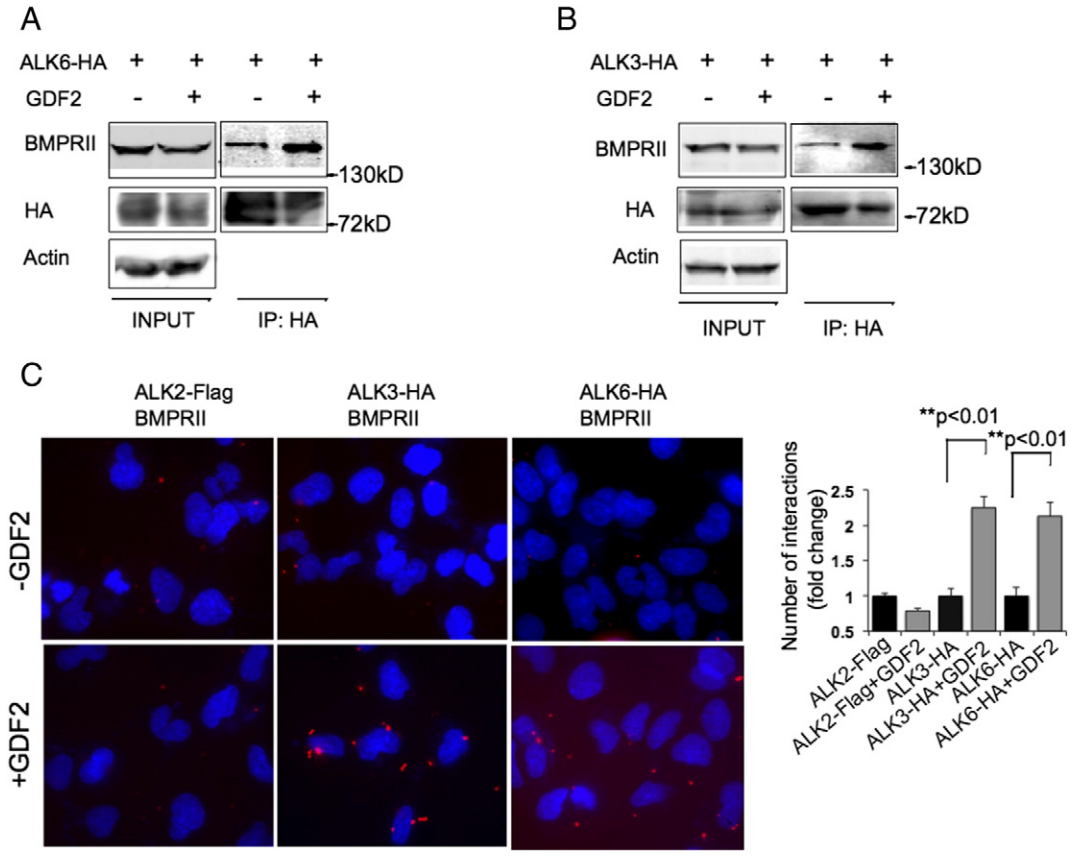

Figure 3. ALK3 and ALK6 interact with BMPRII upon treatment with GDF2. (A-B) HEK293 cells expressing either (A) ALK6-HA or (B) ALK3-HA with or without stimulation for 30 minutes with GDF2 were lysed, immunoprecipitated with anti-HA, and immunoblotted for endogenous BMPRII and HA as indicated with assessment of 10% of the protein lysate for input. Actin was the loading control. (C-D) GDF2 specifically increases BMPRII-ALK3 and BMPRII-ALK6 interaction. Fluorescent images of proximity ligation in PA1 cells between ALK3-HA, ALK6-HA, or ALK2-Flag, with endogenous BMPRII, with or without GDF2 as described in methods. Dots are representative of protein proximity and interaction. (D) Quantification of the interaction compared with control cells is presented. In PA1 cells, protein interaction increased two-fold (**$P < .01$) in the ALK3-HA– and ALK6-HA–expressing cells; $N = 50$ per condition.

proliferation and to investigate whether inhibition of apoptosis would offer a survival advantage in the presence of GDF2, we measured acini size in the presence and absence of GDF2 over a period of 10 days and in the presence or absence of pan-caspase inhibition. A significant decrease in acini size in GDF2 treated cells was observed (***$P < .001$; Figure 4*C*) that was partially rescued when apoptosis inhibition was combined with GDF2 treatment (***$P < .001$). These data indicate that acini in the presence of GDF2 induce anoikis significantly more rapidly than control cells consistent with early and increased activation of cleaved caspase 3 in response to GDF2 (Figure 4*A*). Interestingly, we observed little to no change in the proliferative capacity of cells treated with GDF2 for up to 5 days and grown under adherent conditions (Supplementary Figure S3, *C* and *D*).

To begin to determine the mechanism by which GDF2 regulated anoikis sensitivity, we asked whether GDF2 induces SMAD1 phosphorylation under anoikis conditions as well. Surprisingly, in both the ovarian and breast epithelial cell lines, GDF2 induced and sustained SMAD1/5 phosphorylation under anoikis (Figure 4*D*) compared with control cells, pointing to a possible link between GDF2-induced sustained SMAD1 activation and anoikis sensitivity.

To investigate the biological significance of ALK3/ALK6/SMAD1 activation in anoikis sensitivity, we carried out the anoikis assay in PA1 cells in the presence of dorsomorphin, which inhibits GDF2-induced SMAD 1/5 phosphorylation (Figure 2*A*). Dorsomorphin treatment suppressed GDF2-induced anoikis sensitivity, as evident from the decrease in levels of CC3 (Figure 5*A*, Supplementary Figure S3*E*), implicating SMAD1 in mediating GDF2-induced anoikis. Because our data have established the involvement of the type I receptors ALK3 and ALK6 in SMAD1/5 phosphorylation (Figure 2), we wanted to evaluate the contribution of ALK3 and ALK6 in GDF2-induced anoikis. Whereas anoikis was evident 24 hours after anchorage-independent growth, dominant negative ALK3 (ALK3 K-R) was able to suppress anoikis more rapidly at the 24-hour time point compared with dominant negative ALK6 (ALK6 K-R). However, compared with mock transfected controls, both ALK3 K-R and ALK6 K-R were able to suppress GDF2-induced anoikis at the 48-hour time point (Figure 5*B*, Supplementary Figure S3*F*). These data collectively indicate that GDF2-induced SMAD1/5 phosphorylation is sustained under anoikis conditions, is required for anoikis sensitivity, and is mediated via ALK3 and ALK6. To confirm the roles of ALK3/ALK6 and SMAD1 in enhancing anoikis sensitivity, we used shRNA to reduce ALK3, ALK6, and SMAD1 and measured anoikis upon GDF2 treatment. We find that GDF2 induced CC3 and cell viability was reduced upon lowering ALK3 and ALK6 levels by shRNA (Figure 5, *C* and *D*). Similarly, GDF2-mediated anoikis was also reduced upon lowering expression of SMAD1 using shRNA

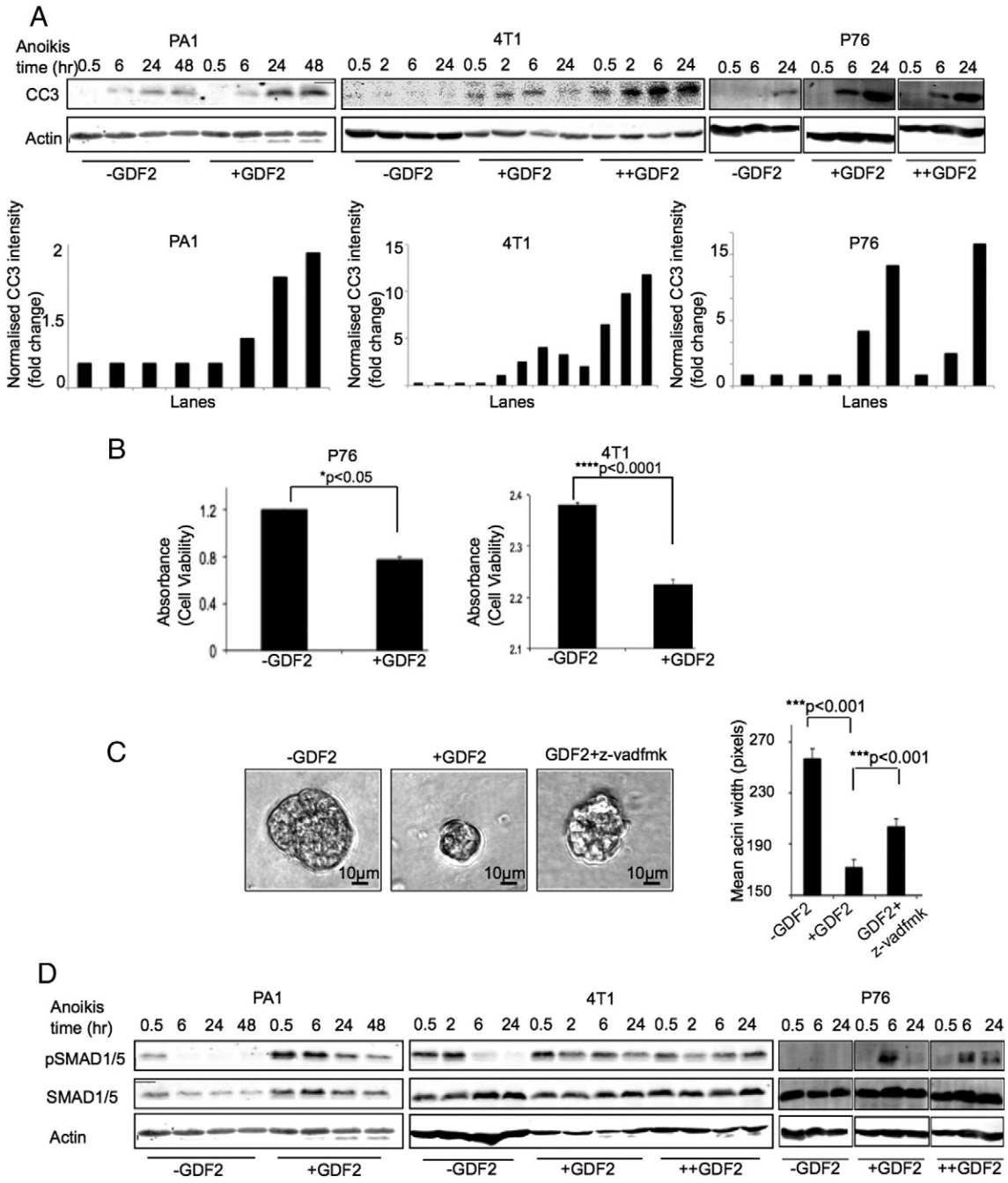

Figure 4. GDF2 stimulates anoikis. (A) Indicated cell lines were plated for anoikis as described in Methods on poly-HEMA–coated plates and treated with either 10 ng/ml (+) or 20 ng/ml (++) of GDF2. Western blotting for CC3 and actin is presented. Normalized densitometry analysis of CC3 intensities is presented below. (B) Absorbance values using the MTT assay (Methods) after anoikis for 24 hours with different concentrations of GDF2 are presented. Data are representative of two independent experiments (*$P < .05$ and ****$P < .0001$ in p76 and 4T1 cells, respectively). Error bars indicate SEM. (C) Acini size of MCF10A cells grown on growth factor reduced Matrigel with or without 20 ng/ml of GDF2 in the presence or absence of pan-caspase inhibitor Z-VAD-FMK for 10 days is presented. Mean acini width is quantified (***$P < .01$). $N = 30$; error bars indicate SEM. (D) Western blotting of same cell lysates prepared as described for (A) was probed for pSMAD1/5 and total SMAD1/5. Actin was the loading control.

to SMAD1 (Figure 5*E*, Supplementary Figure S3*G*). Although our studies point to a role for SMAD1 in GDF2-mediated anoikis, GDF2 has been shown to use non-SMAD mechanisms such as TAK1 (TGFβ activated kinase) to activate endothelial specific genes [41]. Thus, to determine if TAK1 was required for GDF2-induced anoikis, we used the TAK1 inhibitor 5Z-7-oxozeaenol (Methods) to test GDF2-mediated anoikis. We find that GDF2-mediated anoikis was not suppressed by TAK1 inhibition (Supplementary Figure S3*H*) but rather was slightly enhanced, suggesting a TAK1-independent role for GDF2 on anoikis. These data collectively point to a central role for the ALK3/ALK6/SMAD1 axis in mediating anoikis.

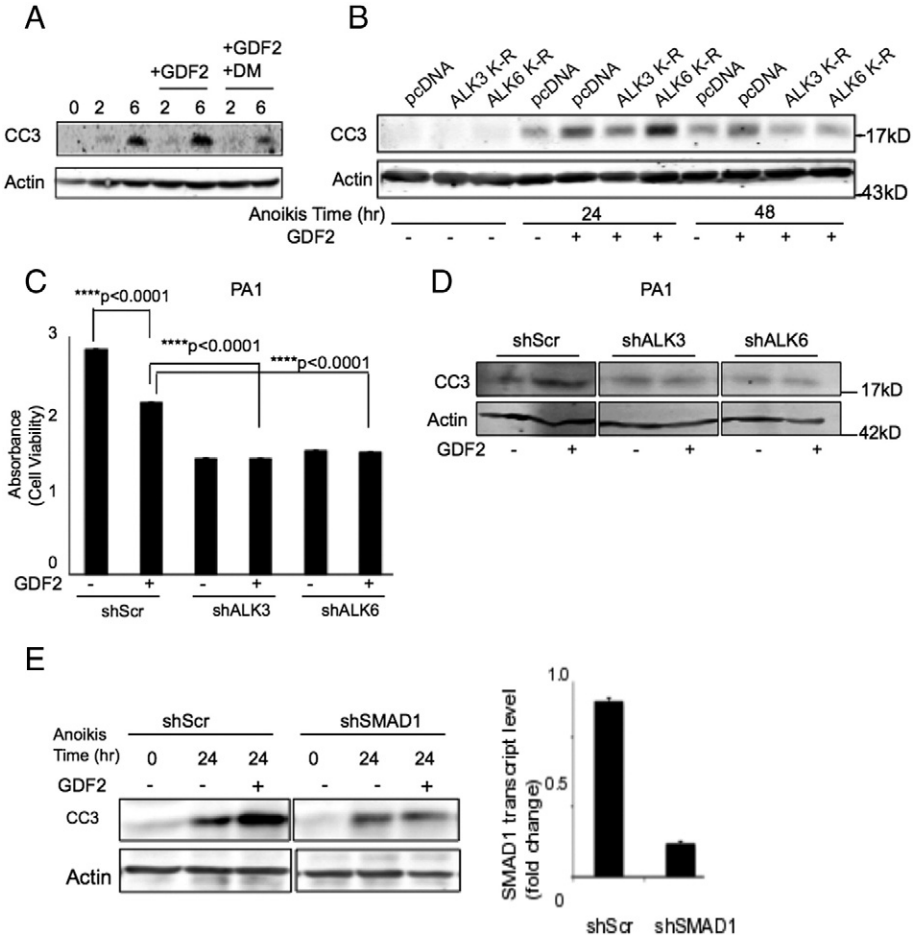

Figure 5. Anoikis susceptibility is mediated via ALK3/ALK6. (A) Western blotting of 4T1 cells grown under anoikis conditions either with or without 1 μM dorsomorphin and GDF2 as indicated. Lysates were immunoblotted against CC3. Actin was the loading control (quantification of CC3 levels presented in Supplementary Figure S3*E*). (B) Kinase mutants ALK3 K-R and ALK6 K-R reduce anoikis. Western blotting of PA1 cells expressing control, ALK3 K-R, or ALK6 K-R was plated for anoikis (Methods) in the absence or presence of GDF2 for indicated times (quantification of CC3 levels presented in Supplementary Figure S3*F*). (C) MTT absorbance values of PA1 cells expressing shScr, shALK3 or shALK6 after 24 hours of anoikis in the absence and presence of 10 ng/ml of GDF2 are presented. Error bars indicate SEM. (D) Western blotting of same cells as in (C) harvested after 24 hours of anoikis and immunoblotted for CC3. Actin was the loading control. (E) Western blotting as indicated of PA1 cells expressing shSMAD1 or shScr at the indicated times under anoikis conditions (quantification of CC3 presented in Supplementary Figure S3*G*). SMAD1 transcript levels upon shRNA to SMAD1 relative to controls are presented in the adjacent graph. Actin was the loading control.

GDF2 Is epigenetically silenced in ovarian and breast epithelial cancers

Our data point to an antitumorigenic function for GDF2 in *in vitro* models of ovarian and breast cancer. We thus wanted to examine if detectable differences exist between protein levels of GDF2 in ovarian and breast cancer cell lines and their transformed counterparts. We used immortalized ovarian surface epithelial cells [42] FTECs [20], MCF10A, and HMEC to represent untransformed cells and compared the level of GDF2 protein levels with six cancer cell lines. Whereas GDF2 protein was observed in all the six untransformed cells, five of the six cancer cell lines tested had no GDF2 protein detectable (Figure 6*A*). Secreted GDF2 protein levels by ELISA also correlated with the transformation status of the cells (Figure 6*B*).

Based on the reduced protein levels and putative roles for GDF2 in increasing anoikis, we hypothesized that GDF2 expression was epigenetically silenced in cell lines and patient samples of ovarian cancer. To determine if GDF2 expression was transcriptionally repressed and if so via recruitment of DNA methyl transferases, we examined GDF2 levels in PA1 cells in the presence or absence of azacytidine (AZA) a strong inducer of protein demethylation [43] (Figure 6*C*). AZA treatment significantly increased GDF2 mRNA levels in a dose- and time-dependent manner, suggesting an epigenetic mechanism in the inactivation of GDF2 gene expression possibly via methylation (Figure 6*C*). To determine whether *GDF2* derepression by AZA treatment would enhance SMAD1/5 phosphorylation in an ALK3- and ALK6-dependent manner, we measured SMAD1/5 phosphorylation under anoikis conditions in the presence of AZA. In accordance with our previous observation on the role of GDF2 and SMAD1 in anoikis, we found that AZA treatment increased SMAD1/5 phosphorylation, CC3, and anoikis sensitivity (Figure 6*D*). Consistent with GDF2-induced anoikis via ALK3/ALK6 (Figure 5) and AZA-induced increase in GDF2 levels and anoikis (Figure 6, *B* and *C*), dorsomorphin treatment inhibited

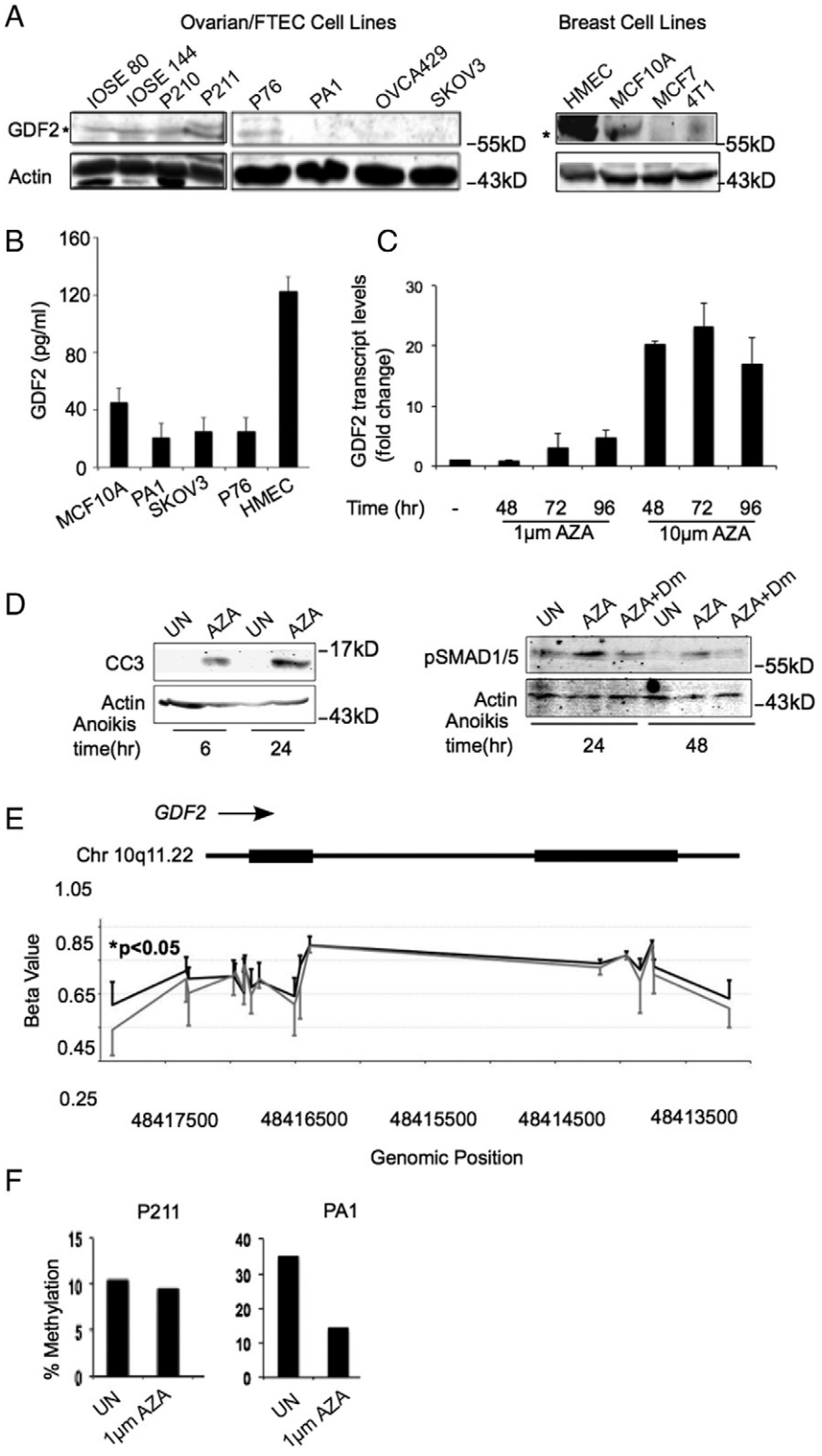

Figure 6. GDF2 expression in breast and ovarian cells. (A) Indicated cell lines were lysed and immunoblotted for GDF2 (*lower band). Actin was the loading control. (B) Secreted GDF2 levels as determined using ELISAs in indicated breast and ovarian cell lines. (C) QRT-PCR levels of GDF2 transcript in the presence of increasing AZA for the indicated time points. Error bars indicate SEM. (D) Western blotting for CC3 and pSMAD1/5 in PA1 cells either untreated or treated with AZA under anoikis conditions for the indicated times. Dorsomorphin (5 μM) was added in combination during anoikis where indicated (Dm). Actin was the loading control. (E) Promoter methylation of *GDF2*. *GDF2* promoter methylation status of ovarian cancer patients ($N = 47$; black line) plotted against normal fallopian tube epithelium (gray line) from the same experiment. Values were plotted using the GraphPad Prism software. Beta values are presented (*$P < .05$). (F) Percent methylation determined by pyrosequencing (Methods and Supplementary Table) of the CpG1 site contained within the *GDF2* promoter in either untransformed P211 or transformed PA1 cells in the presence or absence of 1 μM AZA is presented.

AZA-induced SMAD1/5 phosphorylation. Interestingly, GDF2 quenching using Alk1-ECD, which has been used as a ligand trap for GDF2 [44,45], dampened the effects of AZA-induced anoikis (Supplementary Figure S3*I*), consistent with increased GDF2 levels in response to AZA (Figure 6*C*). These data indicate that methylation-mediated reduction in GDF2 expression may lead to anoikis resistance in cancer.

To extend our findings on GDF2 repression in cancer cell lines, we examined the methylation status of the GDF2 promoter in ovarian cancer patients. We plotted HumanMethylation450 BeadChip beta values using a methodology previously described [23] for a panel of 47 high-grade advanced-stage serous epithelial ovarian cancers and 4 normal fallopian tube fimbriae epithelium specimens across the *GDF2* locus (Figure 6*E*). *GDF2* was more highly methylated (*up to 15% increase $*P < .05$) in the *GDF2* promoter region of tumors from ovarian cancer patients ($n = 47$) as compared with the fallopian tube fimbriae epithelium of normal individuals (Figure 6*E*). These data point to increased DNA methylation in serous ovarian cancer compared with normal precursor cells consistent with its putative role as a tumor-suppressing factor in these cancers. To experimentally validate our finding on the methylation status of the *GDF2* promoter, we carried out pyrosequencing analyses of the same CpG1 site in nononcogenic P211 where GDF2 expression was detected (Figure 6*A*) and PA1 cells that had little to no detectable GDF2 (Figure 6*A*) and investigated whether AZA treatment would reduce methylation at the CpG1 site within the *GDF2* promoter (Figure 6*E**). We find that methylation levels decreased in the ovarian cancer cell line PA1 following AZA treatment (Figure 6*F*) consistent with increased expression of GDF2 upon AZA treatment (Figure 6*C*). Control, untransformed FTEC P211 cells that already express GDF2 (Figure 6*A*) showed no methylation regulation in the presence of AZA. These data indicate that GDF2 expression is repressed by promoter methylation in patient samples and cancer cell lines (Figure 6) and that reexpression can trigger SMAD1/5 signaling and anoikis sensitivity (Figure 6*D*, Supplementary Figure S3*I*).

Discussion

Our study shows for the first time a role for GDF2-induced SMAD1/5 activation via ALK3/ALK6 during anoikis in breast and ovarian epithelial models (Figure 1, *A* and *B*). Although BMP10 bears sequence similarity with GDF2 and is a functional equivalent in binding the type I receptor ALK1 [6,15], BMP10 activation of the SMAD1/5 pathway is significantly less compared with the extent and kinetics of SMAD1/5 activation by GDF2 (Figure 1, *F*, *right panel*). This distinction is rather significant and may explain the similar yet disparate roles of GDF2/BMP9 and BMP10 in cardiac development as well [4]. Although ALK3- and ALK6-dependent BMP10 activity has been observed in osteoblast precursor cells [46], it is likely that lineage-specific utilization of specific type I receptors or ligand heterodimerization may account for this variability [47]. Our data are also supportive of an ALK1-independent tumor suppressive role for GDF2 consistent with *in vivo* studies in breast cancer [14].

The role of GDF2 in tumorigenesis is somewhat unclear because it has been shown to promote ovarian cancer cell growth [16], suppress breast tumorigenesis [48], and increase hepatocellular carcinoma cell growth [13]. The mechanisms behind these pleiotropic effects remain largely unknown. Elucidating the specific biological outcomes and the receptor signaling mechanisms mediated by GDF2 may shed light on the contexts under which GDF2 is a tumor promoter or a suppressor. Previously, ALK2 has been shown to interact with GDF2 [16]; however, our studies indicate a strong preference for ALK3 to induce SMAD1 activation when expressed at equal or higher levels than ALK2, pointing to possible tissue/cancer-specific or type I receptor (ALK)–specific roles for GDF2 that may dictate tumor growth and response. The molecular determinants that drive subtype-specific receptor interaction in response to GDF2 cannot be ascertained from mRNA levels of the type I and type II receptors alone (Supplementary Figure S2*A*). Posttranslational modification and subsequent protein stabilization as in the case of ALK3 might contribute to preferential interaction and outcome [49]. Although this study examines the role of ALK3 and ALK6 in GDF2-mediated signaling and anoikis, the contribution of individual receptor subtype has not been elucidated. Context-dependent precedence of ALK3 or ALK6 might mediate specific signaling and function.

Ovarian cancer aggressiveness has been associated with anoikis resistance, a mechanism adopted by neoplastic cells to evade cell death [38]. Similarly, in breast cancer, ductal carcinoma *in situ* exhibits filling of the epithelial lumen indicating anoikis resistance as an early event in initiation [50]. Accordingly, our data also show anoikis sensitivity in response to GDF2 treatment and anoikis evasion upon ALK3, ALK6, and SMAD1/5 inhibition (Figures 4 and 5). Further studies to examine the precise mechanism used to induce anoikis upon SMAD1/5 activation are warranted.

In our studies, we combined normal and transformed counterparts to assess if GDF2 played differential effects depending on the transformation status. We however saw no significant distinction in signaling responsiveness in our breast and ovarian cancer models based on transformation status. In contrast, there was a correlation between the reduced expression of GDF2 and the transformation status of breast and ovarian cell lines. Neoplastic cells have been shown to contain regions of hypermethylation in tumor suppressor genes. Consistently, GDF2 promoter was methylated in ovarian cancer patients at the CpG1 site, which was experimentally confirmed from our pyrosequencing analyses in our cell line panel (Figure 6*F*). Gene expression can be controlled by multiple mechanisms over and above methylation including histone modifications. Although our data clearly demonstrate a role for methylation in the control of GDF2 expression, it is unlikely the whole story, and future in-depth studies on the control of GDF2 expression in patient populations are warranted.

Our data provide new evidence on the role of GDF2 in cancers of the breast and ovary/fallopian tube. It is interesting to note that despite the low levels of GDF2 in the transformed cells (Figure 6, *A* and *B*), the cells are competent to initiate downstream effectors upon GDF2 treatments like their normal counterparts. Thus, GDF2 treatment or its reactivation could activate signaling sensitivity to mediate anoikis sensitivity in cancer cells (Figure 6*D*). Prior studies examining ovarian cancer tissues have revealed GDF2 staining in 25% of epithelial ovarian cancer with varying expression levels within the epithelial ovarian cancer subtype. Nonepithelial ovarian tumors do not express GDF2 [16]. Analyses of mRNA levels in breast cancer and the adjacent tissues have also revealed increased GDF2 expression in the adjacent nontumor tissues. Such distinctions in GDF2 expression between cancer subtype and proximity may correlate to tumor stage or metastasis [14].

One of the most recent and consistent finds from high-throughput screens in primary human tumor samples has been the high frequencies with which genes encoding epigenetic regulators are

mutated [51]. Although histone demethylase inhibitors are showing promise as targets in the treatment of cancer [52,53], tumorigenicity and metastasis were markedly suppressed when treated with Trichostatin (TSA) and Azacytidine (AZA) in xenograft mouse models of ovarian cancer [54]. From our findings, it is plausible that GDF2 reexpression may play a partial role in sensitizing tumor cells to epigenetic modifier-based therapies and could be complementary to the common targets of cell proliferation and apoptosis.

Supplementary data to this article can be found online at http://dx.doi.org/10.1016/j.neo.2015.11.003.

Acknowledgements

This work was funded in part by the Ovarian Cancer Research Fund grant # 258785, NIGMS/COBRE grant 5P20GM109091-02 to K. M., and the Gail Parkins Ovarian Cancer Awareness fund for S. K. M.

References

[1] Elliott RL and Blobe GC (2005). Role of transforming growth factor beta in human cancer. *J Clin Oncol* **23**(9), 2078–2093.

[2] Miyazono K, Kamiya Y, and Morikawa M (2010). Bone morphogenetic protein receptors and signal transduction. *J Biochem* **147**(1), 35–51.

[3] Laux DW, Young S, Donovan JP, Mansfield CJ, Upton PD, and Roman BL (2013). Circulating Bmp10 acts through endothelial Alk1 to mediate flow-dependent arterial quiescence. *Development* **140**(16), 3403–3412.

[4] Chen H, Brady Ridgway J, Sai T, Lai J, Warming S, Chen H, Roose-Girma M, Zhang G, Shou W, and Yan M, et al (2013). Context-dependent signaling defines roles of BMP9 and BMP10 in embryonic and postnatal development. *Proc Natl Acad Sci U S A* **110**(29), 11887–11892.

[5] Scharpfenecker M, van Dinther M, Liu Z, van Bezooijen RL, Zhao Q, Pukac L, Lowik CW, and ten Dijke P, et al (2007). BMP-9 signals via ALK1 and inhibits bFGF-induced endothelial cell proliferation and VEGF-stimulated angiogenesis. *J Cell Sci* **120**(Pt 6), 964–972.

[6] David L, Mallet C, Mazerbourg S, Feige JJ, and Bailly S (2007). Identification of BMP9 and BMP10 as functional activators of the orphan activin receptor-like kinase 1 (ALK1) in endothelial cells. *Blood* **109**(5), 1953–1961.

[7] Suzuki Y, Ohga N, Morishita Y, Hida K, Miyazono K, and Watabe T (2010). BMP-9 induces proliferation of multiple types of endothelial cells *in vitro* and *in vivo*. *J Cell Sci* **123**(Pt 10), 1684–1692.

[8] Castonguay R, Werner ED, Matthews RG, Presman E, Mulivor AW, Solban N, Sako D, Pearsall RS, Underwood KW, and Seehra J, et al (2011). Soluble endoglin specifically binds bone morphogenetic proteins 9 and 10 via its orphan domain, inhibits blood vessel formation, and suppresses tumor growth. *J Biol Chem* **286**(34), 30034–30046.

[9] Kang Q, Sun MH, Cheng H, Peng Y, Montag AG, Deyrup AT, Jiang W, Luu HH, Luo J, and Szatkowski JP, et al (2004). Characterization of the distinct orthotopic bone-forming activity of 14 BMPs using recombinant adenovirus-mediated gene delivery. *Gene Ther* **11**(17), 1312–1320.

[10] Lopez-Coviella I, Berse B, Krauss R, Thies RS, and Blusztajn JK (2000). Induction and maintenance of the neuronal cholinergic phenotype in the central nervous system by BMP-9. *Science* **289**(5477), 313–316.

[11] Miller AF, Harvey SA, Thies RS, and Olson MS (2000). Bone morphogenetic protein-9. An autocrine/paracrine cytokine in the liver. *J Biol Chem* **275**(24), 17937–17945.

[12] Song JJ, Celeste AJ, Kong FM, Jirtle RL, Rosen V, and Thies RS (1995). Bone morphogenetic protein-9 binds to liver cells and stimulates proliferation. *Endocrinology* **136**(10), 4293–4297.

[13] Herrera B, Garcia-Alvaro M, Cruz S, Walsh P, Fernandez M, Roncero C, Fabregat I, Sanchez A, and Inman GJ, et al (2013). BMP9 is a proliferative and survival factor for human hepatocellular carcinoma cells. *PLoS One* **8**(7), e69535.

[14] Wang K, Feng H, Ren W, Sun X, Luo J, Tang M, Zhou L, Weng Y, He TC, and Zhang Y, et al (2011). BMP9 inhibits the proliferation and invasiveness of breast cancer cells MDA-MB-231. *J Cancer Res Clin Oncol* **137**(11), 1687–1696.

[15] Brown MA, Zhao Q, Baker KA, Naik C, Chen C, Pukac L, Singh M, Tsareva T, Parice Y, and Mahoney A, et al (2005). Crystal structure of BMP-9 and functional interactions with pro-region and receptors. *J Biol Chem* **280**(26), 25111–25118.

[16] Herrera B, van Dinther M, Ten Dijke P, and Inman GJ (2009). Autocrine bone morphogenetic protein-9 signals through activin receptor-like kinase-2/Smad1/Smad4 to promote ovarian cancer cell proliferation. *Cancer Res* **69**(24), 9254–9262.

[17] Ross S and Hill CS (2008). How the Smads regulate transcription. *Int J Biochem Cell Biol* **40**(3), 383–408.

[18] Ren W, Liu Y, Wan S, Fei C, Wang W, Chen Y, Zhang Z, Wang T, Wang J, and Zhou L, et al (2014a). BMP9 inhibits proliferation and metastasis of HER2-positive SK-BR-3 breast cancer cells through ERK1/2 and PI3K/AKT pathways. *PLoS One* **9**(5), e96816.

[19] Lee Y, Miron A, Drapkin R, Nucci MR, Medeiros F, Saleemuddin A, Garber J, Birch C, Mou H, and Gordon RW, et al (2007). A candidate precursor to serous carcinoma that originates in the distal fallopian tube. *J Pathol* **211**(1), 26–35.

[20] Jazaeri AA, Bryant JL, Park H, Li H, Dahiya N, Stoler MH, Ferriss JS, and Dutta A, et al (2011). Molecular requirements for transformation of fallopian tube epithelial cells into serous carcinoma. *Neoplasia* **13**(10), 899–911.

[21] Imamura T, Takase M, Nishihara A, Oeda E, Hanai J, Kawabata M, and Miyazono K, et al (1997). Smad6 inhibits signalling by the TGF-beta superfamily. *Nature* **389**(6651), 622–626.

[22] Debnath J, Muthuswamy SK, and Brugge JS (2003). Morphogenesis and oncogenesis of MCF-10A mammary epithelial acini grown in three-dimensional basement membrane cultures. *Methods* **30**(3), 256–268.

[23] Yamaguchi K, Huang Z, Matsumura N, Mandai M, Okamoto T, and Baba T, et al (2014). Epigenetic determinants of ovarian clear cell carcinoma biology. *Int J Cancer* **135**(3), 585–597.

[24] Murphy SK, Huang Z, and Hoyo C (2012). Differentially methylated regions of imprinted genes in prenatal, perinatal and postnatal human tissues. *PLoS One* **7**(7), e40924.

[25] Attisano L, Carcamo J, Ventura F, Weis FM, Massague J, and Wrana JL (1993). Identification of human activin and TGF beta type I receptors that form heteromeric kinase complexes with type II receptors. *Cell* **75**(4), 671–680.

[26] Zeuthen J, Norgaard JO, Avner P, Fellous M, Wartiovaara J, Vaheri A, Rosen A, and Giovanella BC, et al (1980). Characterization of a human ovarian teratocarcinoma-derived cell line. *Int J Cancer* **25**(1), 19–32.

[27] Holtzhausen A, Golzio C, How T, Lee YH, Schiemann WP, Katsanis N, and Blobe GC, et al (2014). Novel bone morphogenetic protein signaling through Smad2 and Smad3 to regulate cancer progression and development. *FASEB J* **28**(3), 1248–1267.

[28] Korchynskyi O and ten Dijke P (2002). Identification and functional characterization of distinct critically important bone morphogenetic protein-specific response elements in the Id1 promoter. *J Biol Chem* **277**(7), 4883–4891.

[29] Hollnagel A, Oehlmann V, Heymer J, Ruther U, and Nordheim A (1999). Id genes are direct targets of bone morphogenetic protein induction in embryonic stem cells. *J Biol Chem* **274**(28), 19838–19845.

[30] ten Dijke P, Yamashita H, Sampath TK, Reddi AH, Estevez M, Riddle DL, Ichijo H, Heldin CH, and Miyazono K, et al (1994). Identification of type I receptors for osteogenic protein-1 and bone morphogenetic protein-4. *J Biol Chem* **269**(25), 16985–16988.

[31] Reinhold WC, Sunshine M, Liu H, Varma S, Kohn KW, Morris J, Doroshow J, and Pommier Y, et al (2012). Cell Miner: a web-based suite of genomic and pharmacologic tools to explore transcript and drug patterns in the NCI-60 cell line set. *Cancer Res* **72**(14), 3499–3511.

[32] Shankavaram UT, Varma S, Kane D, Sunshine M, Chary KK, Reinhold WC, Pommier Y, and Weinstein JN, et al (2009). Cell Miner: a relational database and query tool for the NCI-60 cancer cell lines. *BMC Genomics* **10**, 277.

[33] Yu PB, Hong CC, Sachidanandan C, Babitt JL, Deng DY, Hoyng SA, Lin HY, Bloch KD, and Peterson RT, et al (2008). Dorsomorphin inhibits BMP signals required for embryogenesis and iron metabolism. *Nat Chem Biol* **4**(1), 33–41.

[34] Inman GJ, Nicolas FJ, Callahan JF, Harling JD, Gaster LM, Reith AD, Laping NJ, and Hill CS, et al (2002). SB-431542 is a potent and specific inhibitor of transforming growth factor-beta superfamily type I activin receptor-like kinase (ALK) receptors ALK4, ALK5, and ALK7. *Mol Pharmacol* **62**(1), 65–74.

[35] Engers DW, Frist AY, Lindsley CW, Hong CC, and Hopkins CR (2013). Synthesis and structure-activity relationships of a novel and selective bone morphogenetic protein receptor (BMP) inhibitor derived from the pyrazolo[1.5-a]pyrimidine scaffold of dorsomorphin: the discovery of ML347 as an ALK2 versus ALK3 selective MLPCN probe. *Bioorg Med Chem Lett* **23**(11), 3248–3252.

[36] Liu F, Ventura F, Doody J, and Massague J (1995). Human type II receptor for bone morphogenic proteins (BMPs): extension of the two-kinase receptor model to the BMPs. *Mol Cell Biol* **15**(7), 3479–3486.

[37] Soderberg O, Gullberg M, Jarvius M, Ridderstrale K, Leuchowius KJ, Jarvius J, Wester K, Hydbring P, Bahram F, and Larsson LG, et al (2006). Direct observation of individual endogenous protein complexes *in situ* by proximity ligation. *Nat Methods* **3**(12), 995–1000.

[38] Cai Q, Yan L, and Xu Y (2014). Anoikis resistance is a critical feature of highly aggressive ovarian cancer cells. *Oncogene* **34**(25), 3315–3324.

[39] Debnath J, Mills KR, Collins NL, Reginato MJ, Muthuswamy SK, and Brugge JS (2002). The role of apoptosis in creating and maintaining luminal space within normal and oncogene-expressing mammary acini. *Cell* **111**(1), 29–40.

[40] Preaudat M, Ouled-Diaf J, Alpha-Bazin B, Mathis G, Mitsugi T, Aono Y, Takahashi K, and Takemoto H, et al (2002). A homogeneous caspase-3 activity assay using HTRF technology. *J Biomol Screen* **7**(3), 267–274.

[41] Park JE, Shao D, Upton PD, Desouza P, Adcock IM, Davies RJ, Morrell NW, Griffiths MJ, and Wort S, et al (2012). BMP-9 induced endothelial cell tubule formation and inhibition of migration involves Smad1 driven endothelin-1 production. *PLoS One* **8**(2), e30075.

[42] Sun Y, Wong N, Guan Y, Salamanca CM, Cheng JC, Lee JM, Gray JW, and Auersperg N, et al (2008). The eukaryotic translation elongation factor eEF1A2 induces neoplastic properties and mediates tumorigenic effects of ZNF217 in precursor cells of human ovarian carcinomas. *Int J Cancer* **123**(8), 1761–1769.

[43] Michalowsky LA and Jones PA (1987). Differential nuclear protein binding to 5-azacytosine-containing DNA as a potential mechanism for 5-aza-2'-deoxycytidine resistance. *Mol Cell Biol* **7**(9), 3076–3083.

[44] Brown FD, Rozelle AL, Yin HL, Balla T, and Donaldson JG (2001). Phosphatidylinositol 4,5-bisphosphate and Arf6-regulated membrane traffic. *J Cell Biol* **154**(5), 1007–1017.

[45] David L, Mallet C, Keramidas M, Lamande N, Gasc JM, Dupuis-Girod S, Plauchu H, Feige JJ, and Bailly S, et al (2008). Bone morphogenetic protein-9 is a circulating vascular quiescence factor. *Circ Res* **102**(8), 914–922.

[46] Mazerbourg S, Sangkuhl K, Luo CW, Sudo S, Klein C, and Hsueh AJ (2005). Identification of receptors and signaling pathways for orphan bone morphogenetic protein/growth differentiation factor ligands based on genomic analyses. *J Biol Chem* **280**(37), 32122–32132.

[47] Butler SJ and Dodd J (2003). A role for BMP heterodimers in roof plate-mediated repulsion of commissural axons. *Neuron* **38**(3), 389–401.

[48] Ren W, Sun X, Wang K, Feng H, Liu Y, Fei C, Wan S, Wang W, Luo J, and Shi Q, et al (2014). BMP9 inhibits the bone metastasis of breast cancer cells by downregulating CCN2 (connective tissue growth factor, CTGF) expression. *Mol Biol Rep* **41**(3), 1373–1383.

[49] Herhaus L, Al-Salihi MA, Dingwell KS, Cummins TD, Wasmus L, Vogt J, Ewan R, Bruce D, Macartney T, and Weidlich S, et al (2014). USP15 targets ALK3/BMPR1A for deubiquitylation to enhance bone morphogenetic protein signalling. *Open Biol* **4**(5), 140065.

[50] Debnath J and Brugge JS (2005). Modelling glandular epithelial cancers in three-dimensional cultures. *Nat Rev Cancer* **5**(9), 675–688.

[51] You JS and Jones PA (2012). Cancer genetics and epigenetics: two sides of the same coin? *Cancer Cell* **22**(1), 9–20.

[52] Liu G, Bollig-Fischer A, Kreike B, van de Vijver MJ, Abrams J, Ethier SP, and Yang ZQ, et al (2009). Genomic amplification and oncogenic properties of the GASC1 histone demethylase gene in breast cancer. *Oncogene* **28**(50), 4491–4500.

[53] Schenk T, Chen WC, Gollner S, Howell L, Jin L, Hebestreit K, Klein HU, Popescu AC, Burnett A, and Mills K, et al (2012). Inhibition of the LSD1 (KDM1A) demethylase reactivates the all-trans-retinoic acid differentiation pathway in acute myeloid leukemia. *Nat Med* **18**(4), 605–611.

[54] Meng F, Sun G, Zhong M, Yu Y, and Brewer MA (2013). Inhibition of DNA methyltransferases, histone deacetylases and lysine-specific demethylase-1 suppresses the tumorigenicity of the ovarian cancer ascites cell line SKOV3. *Int J Oncol* **43**(2), 495–502.

[55] David L, Mallet C, Vailhe B, Lamouille S, Feige JJ, and Bailly S (2007). Activin receptor-like kinase 1 inhibits human microvascular endothelial cell migration: potential roles for JNK and ERK. *J Cell Physiol* **213**(2), 484–489.